

ONE-LOOP MATRIX ELEMENTS FOR FOUR-POINT OFF-SHELL FEYNMAN DIAGRAMS WITH TWO EXTERNAL HEAVY QUARKS AND THREE EXTERNAL LIGHT PARTONS UP TO $O(\epsilon^2)$

Z. Merebashvili

*Inst. of High Energy Physics, Iv. Javakishvili Tbilisi State University,
University Str. 9, 0109, Tbilisi, Georgia*

Abstract:

In the present article we report on the calculation of analytical results of the one-loop amplitudes up to $O(\epsilon^2)$ relevant for the next-to-next-to-leading-order (NNLO) quark-parton model description of the hadroproduction of heavy quarks .

We have analytically evaluated the relevant off-shell master scalar integrals as well as corresponding matrix elements of up to a maximum of 4-point off-shell function level in $d=4-2\epsilon$ dimension. These one-loop amplitudes can also be used as input in the determination of the corresponding NNLO cross sections for heavy flavor photoproduction and in photon-photon reactions

Keywords: *Quantum Chromodynamics, Collider Physics, Next-to-leading order corrections, Polarized processes.*

PACS numbers: 12.38.Bx, 13.85.-t, 13.85.Fb, 13.88.+e

I. INTRODUCTION

It has been already 25 years since the next-to-leading-order (NLO) corrections to the hadroproduction of heavy flavors were first presented in the seminal work [1]. These results were confirmed yet in another seminal work [2].

In the past few years there was much progress in describing the experimental results on heavy-flavor production. For instance, in a recent work [3] it was shown that a NLO analysis of the transverse-momentum distributions does in fact properly describe the latest bottom quark production data [4] in a surprisingly large kinematical range. The improvement in the theoretical prediction is mainly due to

advances in the analysis of parton distribution functions and the QCD coupling constant. Data on top-quark pair production also agrees with the NLO prediction within theoretical and experimental errors (see e.g. Ref. [5]). However, in all the NLO calculations there remains, among others, the problem that the renormalization and factorization scale dependences render the theoretical predictions to have much larger uncertainties than today's standards require. This calls for a next-to-next-to-leading-order (NNLO) calculation of heavy-quark production in hadronic collisions. In fact, the scale dependence of the theoretical prediction is expected to be considerably reduced when NNLO partonic amplitudes are folded with the available NNLO parton distributions. For example, by calculating the inclusive top pair hadroproduction one finds a NNLO scale uncertainty of about 3% [6], which is below the parton distribution uncertainty and in line with the present experimental error [7].

In view of a recent discovery of the Higgs boson at the CERN Large Hadron Collider (LHC) [8], as well as anticipated searches for new physics beyond the standard model, precise phenomenological calculations of heavy-quark production processes become of utmost importance. For they constitute an irreducible background and need to be taken into account when the Higgs boson properties are determined or new physics is being explored.

Several years ago the NNLO contributions to hadron production were calculated by several groups in massless QCD (see e.g. Ref. [9] and references therein). The completion of a similar program for processes that involve massive quarks requires much more dedication, since the inclusion of an additional mass scale dramatically complicates the whole calculation.

At the lower energies of Tevatron II, top-quark pair production is dominated by $q\bar{q}$ annihilation (85%). The remaining 15% comes from gluon fusion. At the higher energies of the LHC, gluon fusion dominates the production process (90%) leaving 10% for $q\bar{q}$ annihilation. This shows that both $q\bar{q}$ annihilation and gluon fusion have to be accounted for in the calculation of top-quark pair production. Since gluon fusion makes up the largest part of the heavy-quark pair production cross section at the LHC it is important to reduce renormalization and factorization scale uncertainties in the gluon fusion process as much as possible in view of the fact that the large uncertainties in the gluonic parton distribution functions translate to large cross section uncertainties at the LHC.

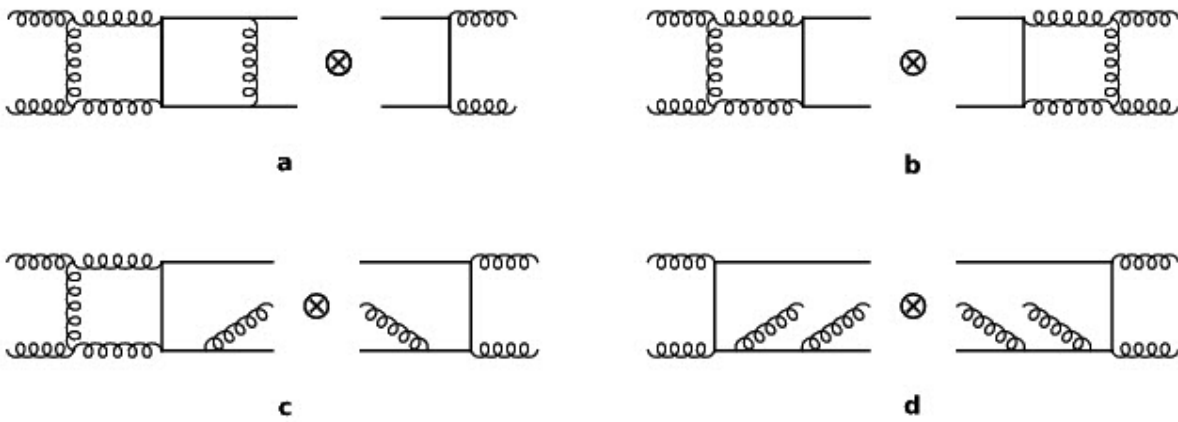


FIG.1: Exemplary gluon fusion diagrams for the NNLO calculation of heavy-hadron production

There are four classes of contributions that need to be calculated for the NNLO corrections to the hadronic production of heavy-quark pairs. In Fig. 1 we show one generic diagram each for the four classes of contributions that need to be calculated for the NNLO corrections to the gluon-initiated hadroproduction of heavy flavors. The first class involves the pure two-loop contribution [1(a)], which has to be folded with the leading-order (LO) Born term. The second class of diagrams [1(b)] consists of the so-called one-loop squared contributions arising from the product of one-loop virtual matrix elements. Further, there are the one-loop gluon emission contributions [1(c)] that are folded with the one-gluon emission graphs. This is the topic of the present paper. Finally, there are the squared two-gluon emission contributions [1(d)] that are purely of tree type. The corresponding graphs for the quark-initiated processes are not displayed.

Bits and pieces of the NNLO calculation for hadroproduction of heavy flavors are now assembled. In this context we would like to mention the recent two-loop calculation of the heavy-quark vertex form factor [10] that can be used as one of the many building blocks in the first class of processes. There is also a numerical approach applied to the calculation of the pure two-loop diagrams [11]. Recently, an analytic calculation of a subclass of the two-loop contributions to $q\bar{q} \rightarrow Q\bar{Q}$ was published [12]. The authors of [13] have calculated the NLO corrections to $t\bar{t}$ +jet production with contributions from the third class of diagrams. However, this result needs further subtraction terms in order to allow for an integration over the full phase space.

Regarding the second class of contributions, all the necessary master scalar integrals

needed in this calculation have been assembled in Ref. [14], with the results expressed in terms of so-called L -functions, which can be written as one-dimensional integral representations involving products of log and dilog functions. Alternatively, in [15] the results for these scalar integrals are rewritten as a multitude of multiple polylogarithms of maximal weight and depth 4. The divergent and finite terms of the one-loop amplitudes for $q\bar{q} \rightarrow Q\bar{Q}$ and $gg \rightarrow Q\bar{Q}$ were given in Ref.[16]. The remaining $O(\varepsilon)$ and $O(\varepsilon^2)$ amplitudes have been written down in Ref.[17]. All these results were presented in a closed analytic form. The NNLO one-loop squared amplitudes for the quark-initiated process were presented in Ref. [18]. The calculation of the NNLO one-loop squared matrix elements for the process $gg \rightarrow Q\bar{Q}$ was done in [19], as well as in [20]. In Refs. [18-20] results for scalar master integrals of [14,15] were used exclusively. The calculation is carried out in dimensional regularization [21] with space-time dimension $n = 4 - 2\varepsilon$. We mention that a closed-form, one-loop squared results for heavy-quark production in the fusion of real photons are presented in Ref. [22].

The available results were collected and correspondingly combined in a semi-numerical calculation of the fully inclusive total cross section for top-quark production in Refs.[6,7].

Let us briefly describe some of the main features of the calculation of the one-loop light parton emission contributions. The highest singularity in the one-loop amplitudes arises from infrared (IR) and mass singularities (M) and is thus, in general, proportional to $(1/\varepsilon^2)$. After folding the one-loop amplitudes with the corresponding tree amplitudes and integrating over the full phase space of the light parton the poles $(1/\varepsilon)$ and $(1/\varepsilon^2)$ will arise. This in turn implies that the Laurent series expansion of the one-loop amplitudes has to be taken up to $O(\varepsilon^2)$ when folding them with the corresponding tree level contributions and subsequently integrating over the phase space of the final partons. All the master scalar integrals given in Ref. [14] will be required in the present calculation. However, due to the complicated kinematics, some new integrals will arise in this case. All additional scalar master integrals needed in this paper have been assembled in Ref.[23]. The aim of our work is to obtain a complete analytical result for the third class of diagrams in Fig. 1, i.e. calculate the various coefficient functions of the corresponding Laurent series expansions.

II. NOTATION

There are four partonic reactions representing the tree one-gluon emission graphs that are to be folded with the one-loop $2 \rightarrow 3$ diagrams of class [1(c)]:

$$\begin{aligned} gg &\rightarrow Q\bar{Q}g, & q\bar{q} &\rightarrow Q\bar{Q}g, \\ gq &\rightarrow Q\bar{Q}q, & \bar{q}g &\rightarrow Q\bar{Q}\bar{q}. \end{aligned} \tag{2.1}$$

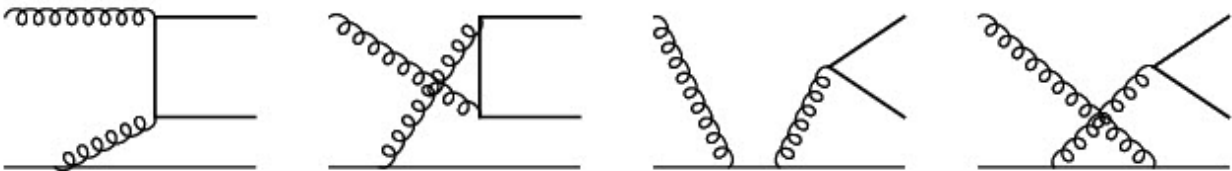


FIG. 2. The lowest order Feynman diagram representing gluon and light (anti)quark collision. In Fig.2 we present an exemplary set of the lowest order tree diagrams for the third reaction above. Apparently, the corresponding virtual diagrams can be obtained from the above graphs by inserting the loops into every line by all possible means. Alternatively, the virtual $2 \rightarrow 3$ graphs for the

gluon fusion reaction can be obtained from the graphs e.g. of Figs. 3 and 4 by insertion of an additional gluon external leg into every 3-gluon vertex, propagator, and external line. The remaining tree $2 \rightarrow 3$ graphs arising at this $O(\alpha_s^2)$ level of a QCD perturbation theory are due to a quark-gluon annihilation subprocess. Note that the last three reactions in (2.1) can be obtained from each other by crossing.

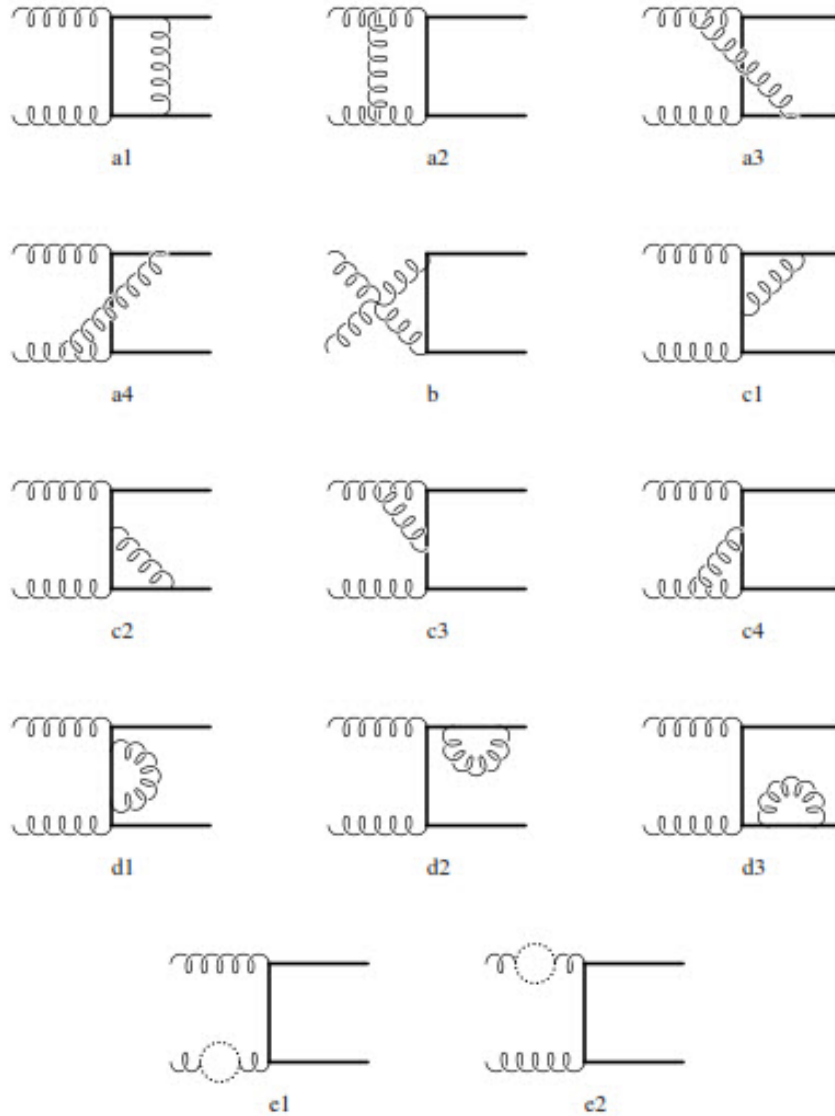


FIG.3. The t channel one-loop graphs contributing to the gluon fusion amplitude. Loops with dotted lines represent the gluon, ghost, and light and heavy quarks

Irrespective of the partons involved, the general kinematics is, of course, the same in all these subprocesses. In general, we have

$$f(\mathbf{p}_1) + f(\mathbf{p}_2) \rightarrow Q(\mathbf{p}_3) + \bar{Q}(\mathbf{p}_4) + f(p_5) \quad (2.2)$$

where f stands for a light parton, e.g. gluon or quark. The momentum flow directions correspond to the physical configuration, i.e. p_1 and p_2 are ingoing whereas p_3 , p_4 and p_5 are outgoing. With m being the heavy-quark mass, one has

$$p_1 + p_2 = p_3 + p_4 + p_5, \quad p_1^2 = p_2^2 = p_5^2 = 0, \quad p_3^2 = p_4^2 = m^2. \quad (2.3)$$

We also define

$$\begin{aligned} s &\equiv (p_1 + p_2)^2, \quad t \equiv T - m^2 \equiv (p_1 - p_3)^2 - m^2, \\ u &\equiv U - m^2 \equiv (p_2 - p_3)^2 - m^2 \end{aligned} \quad (2.4)$$

In our presentation, we shall make use of our notation for the coefficient functions of the relevant scalar one-loop master integrals calculated up to $O(\varepsilon^2)$ in Refs. [14,15,23]. Taking the *complex* scalar three-point function C_i as an example, we define successive coefficient functions $C_i^{(j)}$ for the Laurent series expansion of C_i .

One has

$$C_i = iC_\varepsilon(m^2) \left\{ \frac{1}{\varepsilon^2} C_i^{(-2)} + \frac{1}{\varepsilon} C_i^{(-1)} + C_i^{(0)} + \varepsilon C_i^{(1)} + \varepsilon^2 C_i^{(2)} + O(\varepsilon^3) \right\}, \quad (2.5)$$

where $C_\varepsilon(m^2)$ is defined by

$$C_\varepsilon(m^2) \equiv \frac{\Gamma(1 + \varepsilon)}{(4\pi)^2} \left(\frac{4\pi\mu^2}{m^2} \right)^\varepsilon \quad (2.6)$$

We use this notation for both the real and imaginary parts of C_i , i.e. for $\text{Re}C_i$ and $\text{Im}C_i$. Similar expansions hold for the scalar one-point function A_i , the scalar two-point functions B_i , and the remaining scalar three-point functions S_i . Thus our task is to define these coefficient functions.

As was shown e.g. in Refs. [16,17] the self-energy and vertex diagrams contain ultraviolet (UV), infrared and collinear (IR/M) poles after heavy-mass renormalization. The UV poles need to be regularized.

Our renormalization procedure is carried out in a mixed renormalization scheme. When dealing with massless quarks, we work in the modified minimal-subtraction (\overline{MS}) scheme, while heavy quarks are renormalized in the on-shell scheme defined by the following conditions for the renormalized external heavy-quark self-energy graphs:

$$\Sigma_r(p) \Big|_{p=m} = 0, \quad \frac{\partial}{\partial p} \Sigma_r(p) \Big|_{p=m} = 0 \quad (2.7)$$

In the on-shell scheme, the first condition in Eq. (2.7) ensures that the heavy-quark mass is the pole mass.

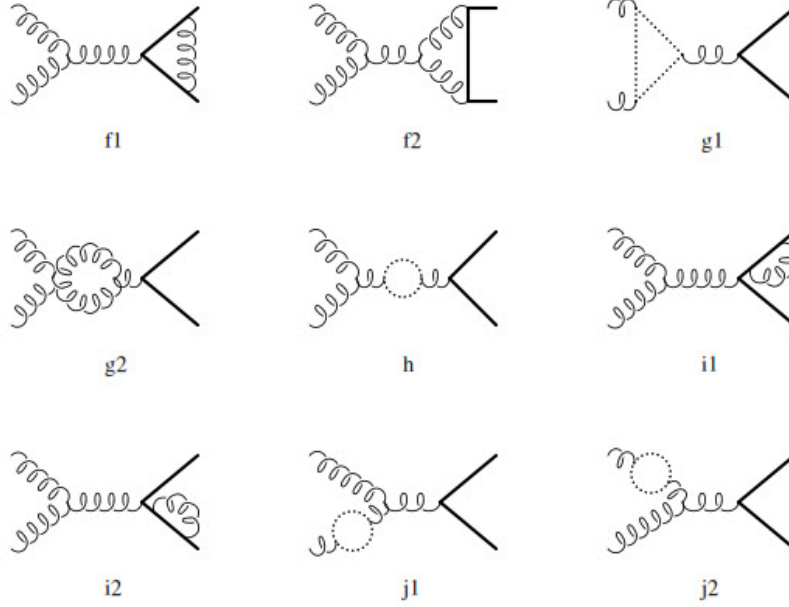


FIG. 4. The s -channel one-loop graphs contributing to the gluon fusion amplitude.

Loops with the dotted lines as in g1, h, j1, and j2 represent the gluon, ghost, and light and heavy quarks. The four-gluon coupling contribution appears in g2.

For completeness, we list the set of one-loop renormalization constants used in this paper. One has

$$\begin{aligned}
 Z_1 &= 1 + \frac{g_s^2}{\epsilon} \frac{2}{3} \left\{ (N_C - n_l) C_\epsilon(m^2) \right\} \\
 Z_m &= 1 - g_s^2 C_F C_\epsilon(m^2) \frac{3 - 2\epsilon}{\epsilon(1 - 2\epsilon)} \\
 Z_2 &= Z_m \\
 Z_{1F} &= Z_2 - \frac{g_s^2}{\epsilon} N_C C_\epsilon(\mu^2) \\
 Z_{1f} &= 1 - \frac{g_s^2}{\epsilon} N_C C_\epsilon(\mu^2) \\
 Z_3 &= 1 + \frac{g_s^2}{\epsilon} \left\{ \left(\frac{5}{3} N_C - \frac{2}{3} n_l \right) C_\epsilon(\mu^2) - \frac{2}{3} C_\epsilon(m^2) \right\} = \\
 &= 1 + \frac{g_s^2}{\epsilon} \left\{ (\beta_0 - 2N_C) C_\epsilon(\mu^2) - \frac{2}{3} C_\epsilon(m^2) \right\} \\
 Z_g &= 1 - \frac{g_s^2}{\epsilon} \left\{ \frac{\beta_0}{2} C_\epsilon(\mu^2) - \frac{1}{3} C_\epsilon(m^2) \right\}
 \end{aligned} \tag{2.8}$$

with $\beta_0 = (11N_C - 2n_l)/3$ being the first coefficient of the QCD beta function, n_l the number of light quarks, $C_F = 4/3$ and $N_C = 3$ the number of colors. The arbitrary mass scale μ is the scale at which the renormalization is carried out. The above renormalization constants renormalize the following quantities: Z_1 for the three-gluon vertex, Z_m for the heavy-quark mass, Z_2 for the

heavy-quark wave function, Z_{1F} for the $(Q\bar{Q}g)$ vertex, Z_{1f} for the $(q\bar{q}g)$ vertex Z_3 for the gluon wave function and Z_g for the strong-coupling constant α_s . For the massless quarks, there is no mass and wave function renormalization.

Let us sketch the two alternative ways of getting the final one-loop-renormalized amplitude from the mass-renormalized amplitude:

i) Take the given mass-renormalized matrix element or the square of that matrix element and multiply all the self-energy graphs by a factor 1/2. Then renormalize the coupling constant in the LO Born amplitude.

ii) Take the given mass-renormalized matrix element and apply the corresponding counterterms obtained from the LO matrix element by inserting the relevant $Z-1$ factors into the *internal* propagators and vertices. All the renormalization constants we need are presented in Eq. (2.8). We will get the renormalized vertex function $\Gamma_R^{(N)}$, where (N) denotes the set of N external particles.

The renormalized matrix element is obtained from

$$M_R = \Gamma_R^{(N)} \prod_{i=1}^N (Z_R^{(i)})^{\frac{1}{2}} \quad (2.9)$$

where $Z_R^{(i)}$ are the residues of the renormalized propagators at the poles for all the particles under consideration. They are related to the residues of the unrenormalized propagators via

$$Z_R^{(i)} = Z_U^{(i)} Z_i^{-1} \quad (2.10)$$

where the Z_i are the respective external wave function renormalization constants.

Working at the one-loop order, we note that in the on-shell scheme $Z_R^{(i)} = 1$. This is a direct consequence of the second condition in Eq (2.7), which effectively cuts off the external massive lines. For the case of external massless partons $Z_U^{(i)} = 1$. It is important to note that the gluon wave function renormalization constant Z_3 is a mixture of two parts: the part which multiplies $C_\epsilon(\mu^2)$ is derived in the \overline{MS} scheme, while the last term due to the heavy-quark loop is derived in the on-shell scheme. For mrenormalization constant in Eq.(2.10). Since in our case we have two gluon and two heavy-quark fields, we therefore obtain

$$M_R = \Gamma_R^{(N)} Z_3^{-1} \quad (2.11)$$

The final result should not depend on which of the two ways has been chosen to do the renormalization. We have checked that, in both ways, one arrives at the same renormalized matrix element.

In order to fix our normalization, we write down the differential cross section for $gg \rightarrow Q\bar{Q}$ in terms of the squared amplitudes $|M|^2$. One has

$$d\sigma_{gg \rightarrow Q\bar{Q}} = \frac{1}{2s} \frac{d(PS)_2}{4(1-\epsilon)^2} \frac{1}{d_A^2} |M|_{gg \rightarrow Q\bar{Q}}^2, \quad (2.12)$$

where the n -dimensional two--body phase space is given by

$$d(PS)_2 = \frac{m^{-2\epsilon}}{8\pi s} \frac{(4\pi)^\epsilon}{\Gamma(1-\epsilon)} \left(\frac{tu - sm^2}{sm^2} \right)^{-\epsilon} \delta(s+t+u) dt du. \quad (2.13)$$

We explicitly exhibit the flux factor $(4p_1 p_2)^{-1} = (2s)^{-1}$, the spin $(n-2)^{-2} = (2-2\epsilon)^{-2}$ and color d_A^{-2} averaging factors for the initial gluons.

Here $d_A = N_C^2 - 1 = 8$ is the dimension of the adjoint

representation of the color group $SU(N_C)$.

III.TWO AND THREE-POINT FUNCTIONS

The one-loop two-point functions are defined by $n = 4 - 2\varepsilon$

$$B(q_1, m_1, m_2) = \mu^{2\varepsilon} \int \frac{d^n q}{(2\pi)^n} \frac{1}{(q^2 - m_1^2) \left[(q + q_1)^2 - m_2^2 \right]}, \quad (3.1)$$

where the $m_i (i = 1, 2)$ can be either m or 0. In the denominators of the relevant functions we always imply the "causal" $+i\delta$ prescription to deal with singularities in pseudo-Euclidean space. The ε -expansion of the two-point functions starts at ε^{-1} . It turns out that $B_i^{(-1)} = 1$ for all i . The general two-point function

$$B_6 \equiv B(q_1, 0, m) \quad (3.2)$$

can be cast into the following compact form:

$$B_6^{(-)} = 1$$

$$B_6^{(0)} = 2 + \frac{m^2 - q_1^2}{q_1^2} \ln \frac{m^2 - q_1^2}{m^2} \quad (3.3)$$

$$B_6^{(1)} = 2B_6^{(0)} - \frac{m^2 - q_1^2}{q_1^2} \ln \frac{m^2 - q_1^2}{m^2} - \frac{m^2 - q_1^2}{q_1^2} Li_2 \left(\frac{q_1^2}{m^2} \right)$$

$$B_6^{(2)} = 2B_6^{(1)} + \frac{m^2 - q_1^2}{q_1^2} \left[\frac{1}{3} \ln^3 \frac{m^2 - q_1^2}{m^2} + 2Li_3 \left(\frac{q_1^2}{q_1^2 - m^2} \right) + Li_3 \left(\frac{q_1^2}{m^2} \right) \right]$$

$$q_1^2 \rightarrow q_1^2 + i\delta$$

The integral B_6 arises for quark self-energy insertions. For the V6 type diagrams, e.g. when quark self-energy loop is inserted into internal propagator of the leading order Born graph, the extra gluon can be radiated from the upper (above loop, then $q_1 = p_2 - p_4$) or lower part (below loop, then $q_1 = p_3 - p_1$) of the graph. Correspondingly,

$$q_1 = p_2 - p_4, \quad m^2 - q_1^2 = 2p_2 p_4;$$

$$q_1 = p_3 - p_1, \quad m^2 - q_1^2 = 2p_1 p_3$$

and all the relevant integrals are real (e.g. no imaginary parts).

For the graphs of type V7, V8 (e.g. quark self-energy loop is inserted into external line of the leading order Born graph), when brems gluon is radiated before the loop

$$q_1 = p_3 + p_5 = p_1 + p_2 - p_4, \quad m^2 - q_1^2 = -2p_3 p_5 = -s + 2p_1 p_4 + 2p_2 p_4$$

$$q_1 = p_4 + p_5 = p_1 + p_2 - p_3, \quad m^2 - q_1^2 = -2p_4 p_5 = -s + 2p_1 p_3 + 2p_2 p_3$$

respectively. When gluon radiates after the loop, this is similar to the NLO case, i.e. such a self-energy graph is subtracted in our renormalization procedure.

The one-loop three-point functions are defined by

$$C(q_1, q_2, m_1, m_2, m_3) = \mu^{2\epsilon} \int \frac{d^n q}{(2\pi)^n} \frac{1}{(q^2 - m_1^2) [(q + q_1)^2 - m_2^2] [(q + q_1 + q_2)^2 - m_3^2]} \quad (3.4)$$

The vertex integrals to be calculated have to be in the form of Eq. (2.5). For our purposes we do not need imaginary parts of the integrals: as the phase space is real, the imaginary parts of the amplitudes will cancel out in the sum of the complex conjugate quantities. With the above notation in mind, the additional and most complicated three-point one-leg-off-shell integrals are:

$$C(-p_3 - p_5, p_1, 0, m, m); \quad (3.5)$$

$$C(-p_1 + p_5, p_3, 0, 0, m) \quad (3.6)$$

Together with the previously calculated scalar integrals, these new functions constitute a full set of the required vertex integrals.

The one-loop four-point functions are defined by

$$D(q_1, q_2, q_3, m_1, m_2, m_3, m_4) = \mu^{2\epsilon} \int \frac{d^n q}{(2\pi)^n} \frac{1}{(q^2 - m_1^2) [(q + q_1)^2 - m_2^2] [(q + q_1 + q_2)^2 - m_3^2] [(q + q_1 + q_2 + q_3)^2 - m_4^2]} \quad (3.7)$$

The required D_1 -type four-point one-leg-off-shell integrals are:

$$D(p_3, -p_1, -p_2, 0, m, m, m); \quad (3.8)$$

$$D(p_4, -p_2, -p_1, 0, m, m, m); \quad (3.9)$$

$$D(p_3, -p_1, -p_2 + p_5, 0, m, m, m); \quad (3.10)$$

$$D(p_4, -p_2, -p_1 + p_5, 0, m, m, m); \quad (3.11)$$

Bearing in mind that the scalar D_1 integral can be expressed as a function of only p_1, p_2 and p_3 momenta, or alternatively via s, t, u variables, one can verify that the first integral above is identical to the D_1 expression, while the second one equals to $D_1(t \rightarrow -2p_2 p_4, u \rightarrow -2p_1 p_4)$. The last two integrals cannot be easily related to the D_1 function and, therefore, had to be reevaluated.

The required D_2 -type four-point one-leg-off-shell integrals are:

$$D(p_1, -p_3, -p_4 - p_5, 0, 0, m, 0); \quad (3.12)$$

$$D(p_2, p_4, p_3 + p_5, 0, 0, m, 0); \quad (3.13)$$

$$D(p_1, -p_3, -p_4, 0, 0, m, 0); \quad (3.14)$$

$$D(-p_2, p_4, p_3, 0, 0, m, 0); \quad (3.15)$$

Because the original D_2 integral was dependent on p_3, p_4 and either p_1 or p_2 , due to the present $2 \rightarrow 3$ kinematics the first two integrals needed to be recalculated. The third one is $D_2(u \rightarrow -2p_1 p_4)$, while the fourth integral above is $D_2(t \rightarrow -2p_2 p_4)$. The eight D_3 -type four-point one-leg-off-shell integrals can be written down analogously.

IV. RESULTS FOR THE MATRIX ELEMENTS

At LO for $gg \rightarrow Q\bar{Q}$, we shall use a representation which differs from the one given in Refs. [16,17]. First note that there are only two independent color structures for this subprocess. The s-channel matrix element is a sum of two parts, each of which is proportional to one of the two independent color structures. We combine terms with the same color structures of the three (e.g. s, t

and u) production channels. Finally, we remove the heavy-antiquark momentum p_4 using energy-momentum conservation and use on-shell conditions for the gluons ($p_1 \cdot \varepsilon_1 = 0$ and $p_2 \cdot \varepsilon_2 = 0$) and the heavy quark ($\bar{u}_3 p_3 = \bar{u}_3 m$). We then obtain the two color-linked LO matrix elements

$$M_{LO,t} = iT^b T^a \hat{M} / t, \quad M_{LO,u} = iT^a T^b \hat{M} / u \quad (4.1)$$

with

$$s\hat{M} = \gamma^\mu p_1 \gamma^\nu s + 2\gamma^\mu p_1^\nu t - 2\gamma^\nu p_2^\mu t - 2\gamma^\nu p_3^\mu s - 2p_1 g^{\mu\nu} t \quad (4.2)$$

It can be verified that the function \hat{M} is $t \leftrightarrow u$ symmetric, and consequently the color-linked Born amplitudes $M_{LO,t}$ and $M_{LO,u}$ turn into one another under $t \leftrightarrow u$.

We then square the full Born matrix element $M_{LO,t} + M_{LO,u}$ and do the spin and color sums to obtain the LO amplitude

$$|M|_{LO}^2 = \frac{d_A}{2} \left(C_F \frac{s^2}{tu} - N_C \right) |\hat{M}|^2 \equiv B, \quad (4.3)$$

where we have factored out a color-reduced Born term $|\hat{M}|^2$, which reads

$$|\hat{M}|^2 = 8 \left\{ \frac{t^2 + u^2}{s^2} + 4 \frac{m^2}{s} - 4 \frac{m^4}{tu} - \varepsilon 2 \left(1 - \frac{tu}{s^2} \right) + \varepsilon^2 \right\} \equiv \hat{B} \quad (4.4)$$

The expression in Eq.(4.3) for the LO amplitude agrees with the well-known result in n dimensions (see e.g. Ref. [2]). Note that, by using the prescription of Ref.[24], we were able to avoid the introduction of ghost contributions which would otherwise arise from the square of the three-gluon coupling amplitude. In our case the prescription of Ref.[24] consists in the use of on-shell conditions for external gluons, i.e. $p_1 \cdot \varepsilon_1 = 0$ and $p_2 \cdot \varepsilon_2 = 0$ and the exclusion of the heavy-antiquark momentum via $p_4 = p_1 + p_2 - p_3$. When squaring amplitudes, we sum over the two helicities of the gluons using the Feynman gauge, i.e. we use

$$\sum_{\lambda=\pm 1} \varepsilon^\mu(\lambda) \varepsilon^\nu(\lambda) = -g^{\mu\nu} \quad (4.5)$$

The use of the framework set up in Ref. [24] has the advantage in the non-Abelian case that one can omit ghost contributions when squaring the amplitudes. Using the above on-shell conditions already at the amplitude level means that one takes full advantage of the gauge invariance of the problem when squaring the amplitudes. Thus, in general, the results for the different channels will not be identical to the ones which would be obtained using 't Hooft-Feynman gauge throughout.

In the present work we build on the programs that were developed in publications [18] and [19]. The total number of diagrams is 354 for the gluon fusion subprocess and 94 for the each of the light quark-initiated partonic processes. In this work we deal with the two-, three- and four-point functions described in the previous section. To reduce tensor integrals to the scalar master integrals we make use of a standard Passarino-Veltman technique. The program is written in REDUCE \cite{reduce}, and is being extended to take into account a great number of additional diagrams that include new off-shell tensor integrals. The results for the matrix elements are too large to be presented here and are stored as files in a REDUCE format.

IV.CONCLUSIONS

We have derived analytical $O(\alpha_s^4)$ NNLO results for the one-loop off-shell contributions to heavy-quark pair production in the hadron-hadron reaction. The corresponding result for photon-photon fusion, as well as the relevant result for the photon-gluon fusion process can be obtained from our present expressions after some color factor adjustments. As concerns hadroproduction of

heavy quarks, the results of the present work comprise a part of a full result. The work on the remaining part that includes the five-point functions is in progress. Our results form part of the NNLO description of heavy-quark pair production relevant for the NNLO analysis of ongoing experiments at the TEVATRON and the LHC.

The present paper deals with unpolarized gluons in the initial state and unpolarized heavy quarks in the final state. Since our results for the original matrix elements contain the full spin information of the process, an extension to the polarized case with polarization in the initial state and/or in the final state including spin correlations would be possible.

Acknowledgments

We would like to thank J.~Gegelia and M.~Kalmykov for useful discussions. The work of Z.M. was supported by the Georgian Shota Rustaveli National Science Foundation through Grant No. FR/11/24.

REFERENCES

1. P.Nason, S.Dawson and R.K.Ellis, Nucl. Phys. (1988) **B303**, 607; Nucl. Phys. (1989); **B327**, 49. (1990); **B335**, 260(E).
2. W.Beenakker, H.Kuijf, W.L.van Neerven, and J.Smith, Phys. Rev.D (1989); **40**, 54. W.Beenakker, W.L.van Neerven, R.Meng, G.A.Schuler and J.~Smith, Nucl. Phys. (1991) **B351**, 507.
3. B.A.Kniehl, G.Kramer, I.Schienbein, and H.Spiesberger, Phys.Rev.D (2008), **77**, 014011;
4. D.Acosta *et al.* (CDF Collaboration), Phys.Rev.D (2005), **71**, 032001; A.~Abulencia *et al* (CDF Collaboration), Phys.Rev.D (2007),**75**, 012010.
5. D.Chakraborty, J.Konigsberg and D.L.Rainwater, Ann. Rev. Nucl. Part. Sci. (2003); **53**, 301.
6. M.Czakon, P.Fiedler and A.Mitov, Phys.Rev.Lett.**110**, (2013), 252004. arXiv:1303.6254 [hep-ph].
7. M.Czakon, M.L.Mangano, A.Mitov and J.Rojo, arXiv:1303.7215 [hep-ph].
8. A.Conway and H.Wenzel, arXiv:1304.5270 [hep-ph].
9. E.W.N.Glover, J.High Energy Phys. **04** (2004) 021.
10. W.Bernreuther, R.Bonciani, T.Gehrmann, R.Heinesch, T.Leineweber,P.Mastrolia and E.Remiddi, Nucl.Phys.706, (2005), 245.
11. M.Czakon, Phys.Lett.B (2008), **664**, 307.
12. R.Bonciani, A.Ferrogliola, T.Gehrmann, D.Maitre and C.Studerus, J.High Energy Phys. (2008) , **07** 129.
13. S.Dittmaier,P. Uwer, and S.Weinzierl, Phys. Rev. Lett. (2007), **98**, 262002.
14. J.G.Korner, Z.Merebashvili and M.Rogal, Phys.Rev. D(2005), **71**,054028.
15. J.G.Korner, Z.Merebashvili and M.Rogal, J.Math.Phys. (2006),**47**, 072302.
16. J.G.Korner and Z.Merebashvili,Phys.Rev. D (2002),**66**, 054023.
17. J.G.Korner, Z.Merebashvili and M.Rogal, Phys.Rev. D(2006), **73**,034030.
18. J.G.Korner, Z.Merebashvili and M.Rogal, Phys.Rev.D(2008), **77**, 094011.
19. B.A.Kniehl, J.G.Korner, Z.Merebashvili and M.Rogal, Phys.Rev.D(2008), **78**, 094013.
20. C.Anastasiou and S.Mert Aybat, arXiv:0809.1355 [hep-ph].
21. C.G.Bollini and J.J.Giambiagi, Phys.\ Lett. (1972); **40B**, 566 G.'t Hooft and M.Veltman, Nucl.\ Phys. (1972); **B44**, 189 J.F.Ashmore, Lett. Nuovo Cimento (1972), **4**, 289.
22. J.G.Korner, Z.Merebashvili and M.Rogal, Phys.Rev. D(2006), **74**, 094006
23. To be published elsewhere.
24. W.C.Kuo, D.Slaven, and B.L.Young, Phys. Rev. D(1988), **37**, 233.
25. A.Hearn, *REDUCE User's Manual Version 3.7* (Rand Corporation,Santa Monica, CA, 1995).

Article received: 2014-03-20